ERNN: A Biologically Inspired Feedforward Neural Network to Discriminate Emotion from EEG Signal

Reza Khosrowabadi, *Student Member, IEEE*, Chai Quek, *Senior Member, IEEE*, Kai Keng Ang, *Member, IEEE*, Abdul Wahab, *Member, IEEE*

***Abstract*— Emotions play an important role in human cognition, perception, decision making, and interaction. This paper presents a six-layer biologically inspired feedforward neural network to discriminate human emotions from EEG. The neural network comprises a shift register memory after spectral filtering for the input layer, and the estimation of coherence between each pair of input signals for the hidden layer. EEG data are collected from 57 healthy participants from eight locations while subjected to audio-visual stimuli. Discrimination of emotions from EEG is investigated based on valence and arousal levels. The accuracy of the proposed neural network is compared with various feature extraction methods and feedforward learning algorithms. The results showed that the highest accuracy is achieved when using the proposed neural network with a type of radial basis function.**

***Index Terms*— Affective computing, arousal-valence plane, EEG-based emotion recognition, functional connectivity.**

I. Introduction

EMOTIONS are not only important in human creativity and intelligence, but also in human rational thinking, decision making, curiosity, and human interaction [1]. Research in emotions involved multidisciplinary areas such as psychology, neuroscience, and affective computing. Although emotions have been studied extensively, the underlying neural mechanisms especially in terms of expression in response to emotional stimuli or perception of them are not studied extensively [2]–[4]. When a person experiences an emotional episode, the cognition process involved in understanding the situation can be distracted or facilitated [5]–[7]. The mechanism of such interactions between emotions and cognition can be investigated using functional and computational models [8]–[13]. In general, these models are designed based on theoretical and experimental works in psychology and neuroscience and follow the related underlying biological mechanism. Subsequently, these architectures are applied to discriminate emotional states. Usually, experimental studies for emotion recognition are based on face, voice, and biosignals features [14]–[18]. Human biosignals are, however, relatively more consistent across cultures and nations than face or voice features [19]. Therefore, using biosignal features would yield more consistent results.

Nevertheless, emotions are psychophysiological phenomena associated with a wide variety of subjective feeling, thus it is difficult to propose a general architecture. Almost all healthy human, however, have similar patterns of cognitive process and physiological stimulation at the same emotional states. Therefore, corresponding biological neural network involved in emotional perception is described. Subsequently, a feedforward neural network for discrimination of emotions is proposed in this paper that could follow the underlying biological and functional mechanism.

Certain brain regions are associated in the processing of emotional stimuli. For instance, according to modern recording studies, the thalamus, amygdala, hippocampus, basal ganglia, insular cortex, and orbitofrontal cortex are involved in emotion perception [20]–[22]. The amygdale is engaged in implicit memory tasks and the hippocampus is usually employed in explicit memory tasks [23]. These studies show that cortical and subcortical regions are involved in emotion regulation [24], [25]. Information of the external world is acquired by sensory receptor cells and transmitted through synapses in neural pathway, spinal cord, peripheral ganglion, and brainstem to the thalamus. The thalamus maps the topography of this information to sensory area of the cortex. Subsequently, the mapped information is interpreted and encoded in neocortex. The encoded information is then classified using a task specific learning structure [26], as it is described in the following paragraph.

The neocortex consists of the grey matter and is organized in the vertical columns of six horizontal layers whereby the first layer is the outmost layer, and the sixth layer is the innermost layer. These six layers are separated by a characteristic distribution of cell types and neuronal connections. The structure of the neocortex is relatively uniform, but there are exceptions of this uniformity such as lack of the fourth layer in motor cortex [27]. Furthermore, the neocortex is divided into the frontal, parietal, occipital, and temporal lobes.

Manuscript received January 9, 2013; revised May 17, 2013; accepted July 26, 2013.

R. Khosrowabadi is with the Center for Computational Intelligence, School of Computer Engineering, Nanyang Technological University, Singapore 639798 (e-mail: reza0004@e.ntu.edu.sg).

C. Quek is with the Division of Computer Science, School of Computer Engineering, Nanyang Technological University, Singapore 639798 (e-mail: ashcquek@e.ntu.edu.sg).

K. K. Ang is with the Institute for Infocomm Research, Agency for Science, Technology and Research, Singapore 138632 (e-mail: kkang@i2r.a-star.edu.sg).

A. Wahab is with the Division of Computer Science, School of Information and Communication Technology, International Islamic University, Kuala Lumpur 50728, Malaysia (e-mail: abdulwahab@iiu.edu.my).

Color versions of one or more of the figures in this paper are available online at http://ieeexplore.ieee.org.

Digital Object Identifier 10.1109/TNNLS.2013.2280271

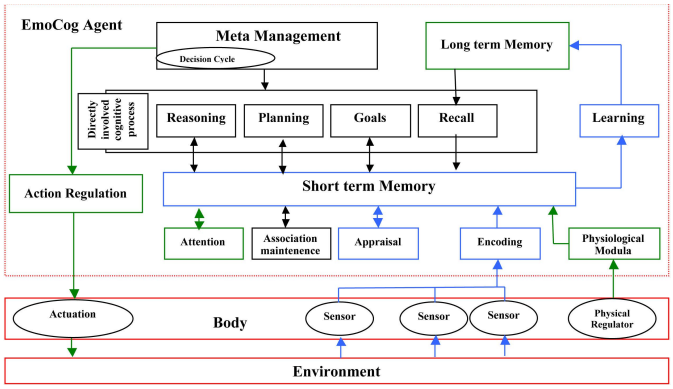

Fig. 1. EmoCog architecture [9].

Each lobe performs a specific function, such as the occipital lobe engages in visual tasks, and the temporal lobe engages in auditory tasks. After the projection of information to the first layer of the primary sensory lobe in the neocortex, the selected information is then transmitted to other sensory areas that ultimately elicit a response. This process includes the segregation of information at the second layer, the estimation of coherence between the patterns at the third layer, and the updating of the memory rate (e.g., speed of motion) at the fifth layer. The attention level to the external stimuli also influences the fourth layer that has direct connections to other layers. After encoding the information, selective attention determines the information to move to short-term memory, and then classifies them based on their meaning, and subsequently stores them in the long-term memory.

Considering the fact that memory is not localized because different memory regions are used for different mental tasks and cognitive function cannot be assigned to any specific part of the brain [28]. Hence, the interactions between the brain regions during the perception of emotional stimuli will be more interpretable if the interactions can be explained functionally.

In general, the functional interactions between the brain regions can be explained using top–down or bottom–up approaches [29]. Perception of emotional stimuli involves a deeper integration so that investigation of both top–down and bottom–up approaches are required [30]. In the top–down approach, emotion is described as a product of a cognitive process that translates the emotional stimuli using appraisal theory [31]. In the bottom–up approach, emotion is explained as a response to stimuli with intrinsic or learned properties and the reinforcement of them [32]. In this paper, top–down approach is computationally modeled. The bottom–up approach is also substituted with subject's feeling. The subject's feeling is based on his/her previous experiences and measured using Self-Assessment Manikin (SAM) [33] questionnaire. Therefore, a biologically inspired model is developed considering both top–down and bottom–up approaches. It is based on a functional model called EmoCog architecture [9] shown in Fig. 1. The EmoCog architecture functionally describes the interaction between the brain regions involved in emotion regulation. This functional model corresponds to the biological brain structure in the outlook of the cognitive process [9]. EEG shows direct brain responses to external stimuli. It carries a lot of information related to translation and encoding of sensory information. Therefore, this signal is acquired during a controlled paradigm to evaluate the computational model.

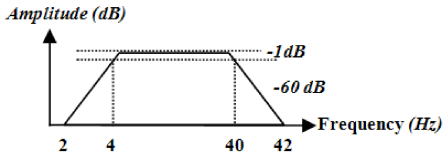

Fig. 2. Spectral filtering.

The remainder of this paper is structured as follows. Section II describes the proposed feedforward neural network for discrimination of emotions from EEG. Section III clarifies the experimental protocol. Section IV presents the experimental results. Section V concludes this paper.

II. Architecture of Proposed Neural Network

The proposed biologically inspired feedforward neural network is shown in Fig. 3.

The neural network is construed to discriminate the emotions from EEG. The process of the emotional states discrimination in each layer of the proposed neural network is described as follows.

A. Functions of Each Layer

This section explains the connectionist architecture of each layer shown in Fig. 3. For convenience of the readers, a list of essential mathematical symbols is shown in Table I.

The multichannel EEG data are the network input and the valence/arousal level is the output.

1) First Layer—Spectral Filtering: EEG signal is often contaminated by noises and artifacts such as ac power-line interference (50 Hz in Singapore), heartbeat, ocular, and muscular artifacts that are mainly located in lower frequencies. A spectral filtering (Fig. 2) is performed on the EEG using a bandpass filter to extract the rhythmic activity from 4 to 40 Hz using

$$X_i^n = \sum_{k=1}^{n} H_i^k E_i^{n-k} \tag{1}$$

where E_i^n denotes the nth sample of the ith channel of the acquired EEG data and X denotes the bandpass filtered data.

The EEG time series after spectral filtering $\mathbf{X} \in \mathrm{R}^{n_p \times n_c}$ are then applied as input to the second layer.

2) Second Layer–A Short-Term Memory: It has been shown in other studies that emotion variations last for some time till the next emotional episode happens, and these variations are detectable using EEG [15]. Therefore, the period of emotional episode represents the use of a short-term memory. Typically, EEG data for a period of 1–4 s is used to discriminate an emotional state [34] because EEG is assumed to remain stationary during short intervals. In the proposed

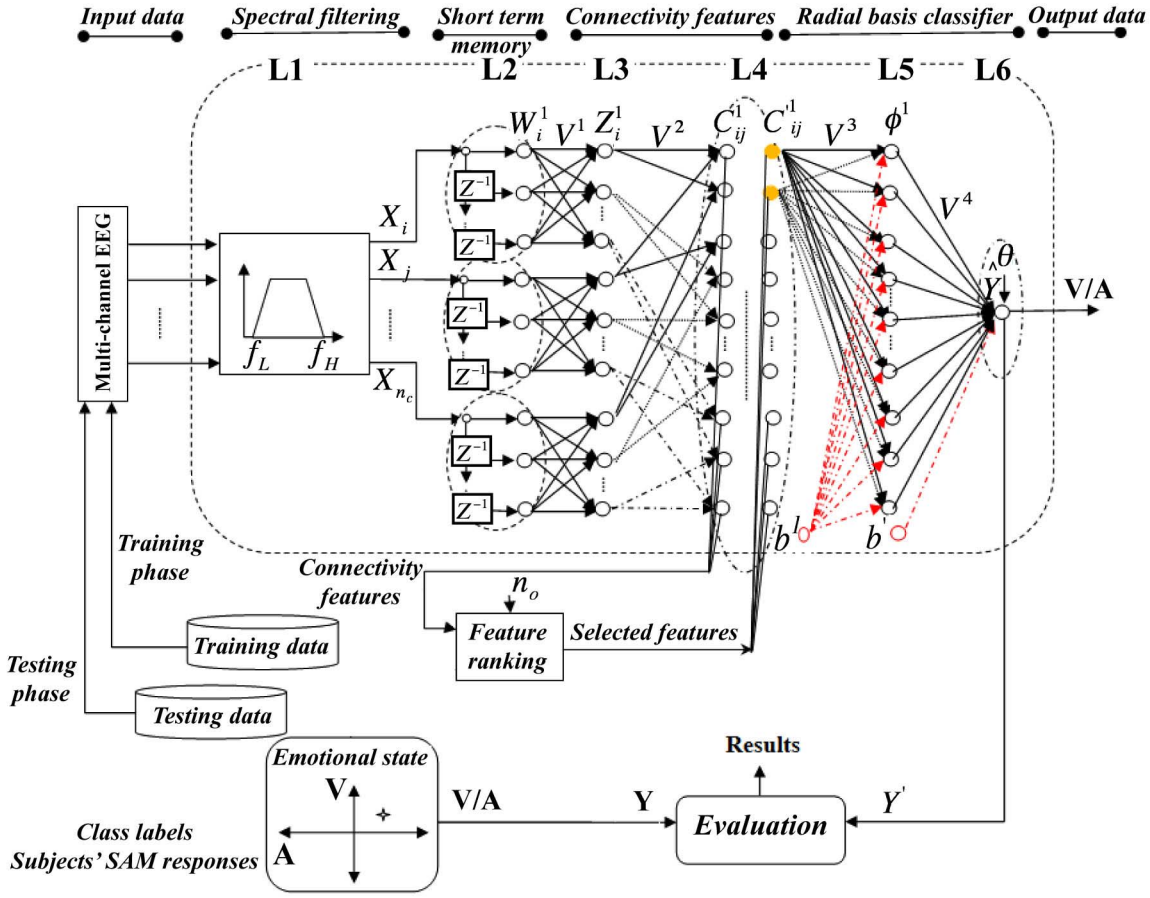

Fig. 3. ERNN: Six-layer feedforward neural network for EEG-based emotion recognition.

neural network, a serial-in/parallel-out shift register memory is used to accumulate the filtered EEG data for a period of 1 s using a rectangular window. The optimum length of EEG data is selected using a genetic algorithm (GA).

The spectral filtered EEG, X, is presented to a rectangular window f_w to produce W. The rectangular window function is calculated using

$$f_w(n) \triangleq \begin{cases} 1 & s_t \le n \le N + s_t \\ 0 & \text{otherwise} \end{cases} \tag{2}$$

$$W_i^n = f_w(n) X_i^n; \qquad \forall n \in [s_t, N + s_t] \tag{3}$$

where $\mathbf{w}_i^n$ denotes the n^{th} sample of the i^{th} channel of windowed filtered EEG and s_t is the start point of window.

W is represented as input to the third layer

$$\mathbf{W} = \left[\mathbf{w}_i, \ldots, \mathbf{w}_{n_c}\right]. \tag{4}$$

3) Third and Fourth Layers—Connectivity Features: Studies have shown that the cortical–subcortical interactions and interaction between different brain regions play an important role in the perception of emotional stimulus [24], [35], [36]. Therefore, brain connectivity features would be very informative to investigate the relationship between emotion and cognition during the perception of emotional stimuli. In addition, the functional connectivity features can overcome the handedness issue because they are not reciprocal [37]. Therefore, the magnitude square coherence estimation (MSCE) [38] is applied to compute the functional connectivity features between the brain regions from EEG signal. To compute the MSCE features, at third layer of the network, the windowed time series EEG, W, is transformed to frequency domain. The MSCE features are then computed in frequency domain with high resolution at the fourth layer.

The weight between n^{th} node of i^{th} channel at second layer and f_i^{th} hidden node at third layer is computed using

$$V_{n_i, f_i}^1 = e^{\frac{-J 2\pi n_i f_i}{N}} \tag{5}$$

where the J denotes the imaginary unit and $e(.)$ is the exponential function.

The transfer function of f_i^{th} hidden node at third layer produces a response $\mathbf{z}_i^f$ given in

$$\mathbf{z}_i^f = \sum_{n=1}^{N} \mathbf{w}_i^n V_{n_i, f_i}^1. \tag{6}$$

After, at fourth layer, the MSCE features [39] are computed using the data transferred to frequency domain Z. The MSCE features are computed for all the pairs of EEG channels in all the frequencies.

The weights between the hidden nodes of third and fourth layers are considered to be one

$$V_{f_i, f_j}^2 = 1, \quad \forall i, \quad j \in \{1, \cdots, n_c\}. \tag{7}$$

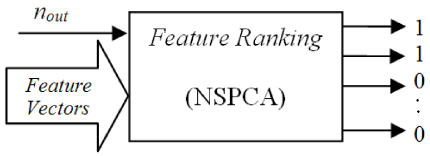

Fig. 4. Hidden nodes selection at third layer.

Because the m^{th} hidden node at fourth layer computes the MSCE between the pairs of $\mathbf{z}_i^f$ and $\mathbf{z}_j^f$, the transfer function for m^{th} hidden node at fourth layer $\mathbf{c}_m^{'f} = \mathbf{c}_{ij}^f$ is computed using

$$\mathbf{c}_m^{'f} = \frac{\left|\mathbf{z}_i^{f^*}\mathbf{z}_j^f\right|^2}{\left(\mathbf{z}_i^f\mathbf{z}_i^{f^*}\right)\left(\mathbf{z}_j^f\mathbf{z}_j^{f^*}\right)} \tag{8}$$

where the $\mathbf{z}_i^{f^*}$ denotes the complex conjugate of the $\mathbf{z}_j^f$.

Some of these extracted features ($\mathbf{c}_m^{'f}$) are, however, irrelevant or redundant and have a negative effect on the accuracy of the classifier. In addition, the structure of neural network at the next layers is chosen based on the number of selected features. Therefore, the network would be very computationally extensive in case of using the huge number of features. Therefore, a number of significant features should be selected. Several supervised and unsupervised methods can be applied. In this paper, nonnegative sparse principal component analysis (NSPCA) is used to extract the significant features in unsupervised manner. NSPCA transforms the original features to a lower dimensional space. This transformation maximizes the variance of the transformed features using parts of the original coordinates and creates a sparse projection [40]. In particular, this method obtains a more biologically grounded decomposition of the data in comparison with the PCA and its application for EEG data analysis has been validated [41].

Initially, the extracted features ($\mathbf{c}_m^{'f}$) are centered by subtracting off the mean. After, the nonnegative principal components of the centered features are calculated. Finally, significant number of features n_{out} are selected. The n_{out} is a constant number and it is one of the network parameters that is selected using an optimization method in this paper. Size of the original features extracted for a subject is $n_f \times n_c^2$, as shown in Table I.

The indexes of most significant features are applied to trigger the outputs of the fourth layer, as shown in Fig. 3 and Fig. 4 using

$$I \in \{0,1\}^{n_{\text{out}}},\ I = f_r(\mathbf{c}', n_{\text{out}}) \tag{9}$$

where $f_r(.)$ denotes the feature ranking function and I denotes the indexes of activated hidden nodes at the fourth layer. The active nodes are shown in orange in Fig. 3. These selected features are the input of fifth layer and computed using

$$C_m^f = I^f C_m^{'f} \ |I^f \neq 0. \tag{10}$$

After, the most significant features are classified using a two layer radial basis function (RBF) type learning algorithm.

TABLE I
LIST OF ESSENTIAL MATHEMATICAL SYMBOLS

Symbol	Description
$\mathbf{X}[n]$	: $\in \mathbb{R}^{n_p \times n_c}$, n_c-channel time series EEG after spectral filtering ; $n \in [1\ n_p]$ $\mathbf{X} = \left[\mathbf{X}_1,\ldots,\mathbf{X}_i,\ldots,\mathbf{X}_{n_c}\right]^T$ where $\mathbf{X}_i \in \mathbb{R}^{n_p \times 1}$ denotes the i^{th} EEG channel
$\mathbf{W}[n]$	: $\in \mathbb{R}^{N \times n_c}$, n_c-channel accumulated EEG using a rectangular window f_w; $n \in [1\ N]$ $\mathbf{W} = \left[\mathbf{W}_1,\ldots,\mathbf{W}_i,\ldots,\mathbf{W}_{n_c}\right]^T$ where $\mathbf{W}_i \in \mathbb{R}^{N \times 1}$ denotes the i^{th} windowed EEG channel
$\mathbf{Z}[f]$	: $\in \mathbb{C}^{N \times n_c}$, Furrier transform of $\mathbf{W}$[n]; $f \in [\frac{F_s}{2 \times N}\ \ \frac{F_s}{2}]$
$\mathbf{C}[f]$	: $\begin{cases} \in \mathbb{R}^{n_f \times n_c^2} \\ 0 \le \mathbf{C}[f] \le 1 \end{cases}$, Coherence feature estimated from pairs of $\mathbf{Z}[f]$; $n_f = \begin{cases} \frac{N}{2}+1, even\ N \\ \frac{N+1}{2}, odd\ N \end{cases}$
$\mathbf{Y}[n]$	: $\in \mathbb{R}^{n_v \times 1}$ or $\in \mathbb{R}^{n_a \times 1}$, valence or arousal class label for $\mathbf{X}[n]$
$V^1_{n_i,f_i}$	: weight between n^{th} node of 2nd layer and f^{th} hidden node of 3rd layer from i^{th} EEG channel
$V^2_{f_i,f_j}$	: weights between $f_i{}^{th}$, $f_j{}^{th}$ hidden node of 3rd layer and $f_{i,j}{}^{th}$ hidden node of 4th layer
V^3_m	: weight vector between hidden nodes of 4th layer and m^{th} hidden node of 5th layer
V^4_m	: weight vector connecting m^{th} hidden nodes of 5th layer to the output node
f_w	: rectangular window function
N	: Size of short term memory (window length)
F_s	: Sampling frequency
f_r	: Feature ranking function
n_i	: n^{th} node of i^{th} EEG channel at second layer
n_v	: Number of subjects for valence level recognition
n_a	: Number of subjects for arousal level recognition
n_c	: Number of EEG channels
n_p	: Number of time samples of EEG
n_{out}	: Number of selected features
n_k	: Number of nearest neighbors
n_h	: Maximum number of nodes at 5th layer
θ	: Hard-threshold calculated from training data
N_a	: Number of added hidden nodes at 4th layer
$b^{'}$	: Bias of output unit
b^1_m	: Bias of m^{th} hidden node at 5th layer

4) Fifth and Sixth Layers—The Classification Stage: After choosing the most significant connectivity patterns between the brain regions, these patterns are correlated to emotional states in a feedforward manner at fifth and sixth layers.

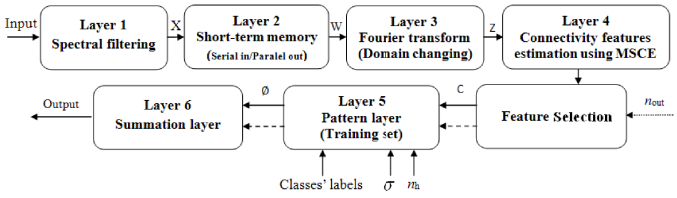

Fig. 5. Phases in the learning process.

According to EmoCog architecture, a one-pass learning algorithm is implemented using a RBF type network. The RBF network is presented in a two-layer structure. The activated hidden nodes at fourth layer (C_m^f) are the input layer of this classifier. Each hidden unit at fifth layer implements a radial activated function. Following the sixth layer, the output unit implements a hard limit function on the weighted sum of fifth layer's hidden units. The transfer functions of hidden nodes at fifth layer are calculated using

$$\phi(V_m^3, C, b_m^1) = g_1\left(b_m^1 \left\| C - V_m^3 \right\|\right) \tag{11}$$

where C denotes the selected features, the b_m^1 denotes the bias of mth hidden node at fifth layer, which is calculated using (12), and $g_1(.)$ is also defined in (13)

$$b_m^1 = \frac{\sqrt{\ln(2)}}{\sigma} \tag{12}$$

$$g_1(X) = e^{-X^T X} \tag{13}$$

where σ denotes the spread of RBFs, $ln(.)$ is a natural logarithm function and $e(.)$ denotes the exponential function.

The output unit function at the sixth layer is also calculated using

$$\hat{Y} = \left(\sum_{m=1}^{\leq n_h} V_m^4 \phi(V_m^3, C, b_m^1)\right) + b' \tag{14}$$

where $\hat{Y}$ denotes the estimated classes labels and the b' denotes the bias of output unit.

In addition, the output of our binary classifier $\hat{\boldsymbol{Y}}$ is assigned to its class label using a hard threshold (step function) using

$$Y' = g_2(\hat{Y}, \theta) = \begin{cases} 1 & \hat{Y} \leq \theta \\ 0 & \hat{Y} > \theta \end{cases} \tag{15}$$

where θ is calculated from training data using

$$\begin{cases} u_1 = \max(\widehat{Y}) \\ u_2 = \min(\widehat{Y}) \end{cases} \rightarrow \theta = \frac{u_1 + u_2}{2}. \tag{16}$$

Initially, the fifth layer does not have any nodes and the hidden nodes of fifth layer are added self-adoptively by orthogonal least square algorithm [42]. The procedure is started by computing the errors associated with input vectors using

$$\boldsymbol{e} = \frac{\left(\left(\boldsymbol{P}' * \boldsymbol{Y}\right)'.\right)^2}{\left(\left(\sum \boldsymbol{Y}. * \boldsymbol{Y}\right)' * \left(\sum \boldsymbol{P}. * \boldsymbol{P}\right)'\right)} \tag{17}$$

where $P = \phi(C', C, b_m^1)$.

Subsequently, the input vector with greatest associated error is detected and a node is added to the fifth layer with weights equal to this vector. The network parameters at the fifth and sixth layers are updated using (18), (20), and (21), respectively

$$\mathbf{V}_{\text{new}}^3 = [\mathbf{V}_{\text{old}}^3, \mathbf{C}'_s] \tag{18}$$

$$\beta = \frac{\mathbf{Y}}{\left[\phi\left(\mathbf{V}_{\text{new}}^{3'}, \mathbf{C}, b^1\right); \text{ones}(1, N_a)\right]} \tag{19}$$

$$\mathbf{V}_{new}^4 = \beta(1 : N_a) \tag{20}$$

$$b'_{new} = \beta(N_a + 1) \tag{21}$$

where Y denotes the desired output of training set and $\mathbf{C}'_s$ is the transpose of the selected vector of C with the greatest associated error. Then, the actual error of network is calculated using mean-square-normalized error. The actual error of network is then compared with defined goal; if the goal has not

TABLE II
INTERSUBJECT CLASSIFICATION ACCURACY FOR EEG-BASED AROUSAL AND VALENCE RECOGNITION

Feature selection , Classification method	*Classification Accuracy*		*Parameters*
	Arousal	*Valence*	
ERNN	**70.83**	**71.43**	$n_h = 2n_a$ *or* $2n_v$ $\sigma = 3.28$,n_{out}=*12*
MSCE-KNN	**62.50**	**62.86**	n_k =*5*
MSCE-ELM(Sig)	**65.22**	**65.71**	Noise at 5th layer=10%
MSCE-SVM	**66.67**	**68.57**	kernel rbf, $\sigma = 6$
MSCE-GRNN	**56.52**	**57.14**	$\sigma = 0.8$
MSCE-NB	**65.22**	**68.57**	
Hj [66]-KNN	**45.83**	**48.57**	n_o=*24*, n_k =n_o
Hj- ELM(Sig)	**54.17**	**51.43**	Noise at 5th layer=10%
Hj- SVM	**47.83**	**54.29**	kernel rbf, $\sigma = 6$
Hj-GRNN	**45.83**	**54.29**	$\sigma = 0.8$
Hj-NB	**47.83**	**51.43**	
FBM-KNN	**47.83**	**54.29**	n_o=*24*, n_k =*5*
FBM-ELM (Sig)	**52.17**	**51.43**	Noise at 5th layer= 10%
FBM-SVM	**54.17**	**54.29**	kernel rbf, $\sigma = 6$
FBM-GRNN	**52.17**	**51.43**	$\sigma = 0.8$
FBM-NB	**47.83**	**51.43**	
GMM_STFT[67]-KNN	**47.83**	**54.29**	n_{cl}=*2*, n_k =*5*
GMM_STFT-ELM(Sig)	**52.17**	**54.29**	Noise at 5th layer=10%
GMM_STFT-SVM	**52.17**	**57.14**	n_{cl}=*2*
GMM_STFT-GRNN	**47.83**	**51.43**	$\sigma = 0.8$
GMM_STFT-NB	**52.17**	**51.43**	
HOC [50]–KNN	**54.17**	**54.29**	n_k =*5*, [8-30]Hz
HOC–KNN	**58.33**	**57.14**	n_k =*5*, [4-40]Hz
HOC –ELM(Sig)	**54.17**	**57.14**	Noise at 5th layer=10%
HOC –SVM	**56.52**	**57.14**	kernel rbf, $\sigma = 6$
HOC –GRNN	**54.17**	**4.29**	$\sigma = 0.8$
HOC –NB	**56.52**	**57.14**	
W_C [51]–KNN	**45.83**	**47.83**	n_k =*5*, [4-68]Hz
W_C –KNN	**54.17**	**51.43**	n_k =*5*, [4-40]Hz
W_C –ELM(Sig)	**42.86**	**47.83**	Noise at 5th layer=10%
W_C –SVM	**56.52**	**57.14**	kernel rbf, $\sigma = 6$
W_C –GRNN	**45.71**	**51.43**	$\sigma = 0.8$
W_C –NB	**54.17**	**54.29**	
MI-KNN	**45.83**	**45.71**	n_k =*5*
MI-ELM(Sig)	**47.83**	**48.57**	Noise at 5th layer=10%
MI-SVM	**52.17**	**48.57**	kernel rbf, $\sigma = 6$
MI-GRNN	**47.83**	**51.43**	$\sigma = 0.8$
MI-NB	**52.17**	**51.43**	
ERNN (All trials)	**65.85±9.73**	**67.3±9.4**	

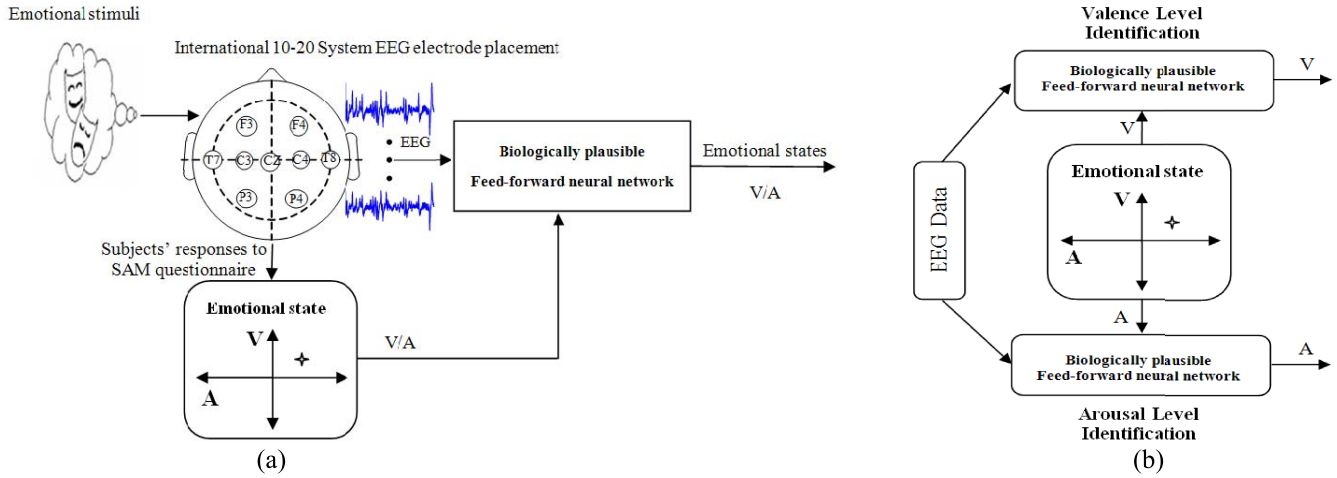

Fig. 6. Protocol of (a) data processing and (b) structure of identification of dynamic parameter of emotions.

been reached, another node is added. This process is continued until the sum squared of actual error falls below the defined goal error or the number of hidden layer nodes at the fifth layer reaches to maximum defined number n_{h}.

B. Learning and Testing Process

The learning process, as shown in Fig. 5, consists of three stages.

1) Computing the parameters of neural network in first, second, third, and fourth layers in an unsupervised manner (computing the MSCE features).
2) Selecting of active hidden nodes in fourth layer using an unsupervised method (NSPCA).
3) Computing the network parameters for fifth and sixth layers in a supervised manner (classification of labeled data).

The binary classes are configured using

$$\begin{cases} Y_v \in \mathrm{N}^{1\times n_v},\ Y_v \in \{0\,,\ 1\} \\ Y_a \in \mathrm{N}^{1\times n_a},\ Y_a \in \{0\,,\ 1\} \end{cases} \tag{22}$$

where Y_v denotes the valence group labels and n_v is the total number of subjects in this group. Similarly, Y_a denotes the arousal group labels and n_a is the number of subjects in this category.

In testing phase, stages 1 and 2 are repeated. The selected features are then classified using parameters calculated in learning phase.

This network is, however, sensitive to value of σ and n_{h}. Furthermore, radial basis networks even when designed efficiently tend to have many times more neurons than other comparable feedforward networks in the hidden layer [43]. These parameters should be tuned properly to lead a high level of accuracy. Nevertheless, network can converge to an optimum accuracy rates by applying a proper value for σ and large enough value for n_{h}. In addition, the RBF network is fast and can be directly implemented in the network [44]. Therefore, other feedforward learning methods are also applied, such as extreme learning machine (ELM) [45], general regression neural network (GRNN) [46], k-nearest neighbor (KNN) method [47], Naive bayesian (NB) [48], and support vector machine (SVM) [49]. The network accuracy using all the mentioned methods is shown in Table II. The results confirm that the RBF network works better than other possible networks. The accuracy of network is also compared with higher order crossing [50] and discrete wavelet transform [51], which are the two existing feature extraction methods for emotion recognition from EEG.

C. Defining the Emotional States—Class Label

Emotion theories and researches have suggested a number of basic emotions although there is no coherent definition [7], [52]–[55]. Basic emotions are defined as the emotions that are common across the cultures and selected by nature because of their high survival factors [55]. Commonly accepted basic emotions include: happy, sad, fear, anger, surprise, disgust, and complex emotions such as shame and disappointment are a combination of these basic emotions [53]. Emotions can also be measured by two axes of valence and arousal plane [53], [56]. Valence measures unpleasant to pleasant, and arousal measures calm to excited levels. Basic emotions can then be mapped onto the valence–arousal space. Different subjects, however, may feel differently while they are exposed to similar emotional stimuli. Therefore, the emotional responses of subjects have to be ascertained using questionnaires. This task is performed using the SAM in this paper. The SAM is a nonverbal pictorial assessment technique that directly measures the valence, arousal, and dominance levels associated with a person's affective reaction to a wide variety of stimuli [57].

The proposed neural network is applied to discriminate the changes of the cognitive process in response to emotional stimuli. These changes are interpreted from the changes in EEG and mapped to subjects' SAM responses in terms of valence and arousal. The process of emotion discrimination from EEG using the proposed neural network is shown in Fig. 6(a). The arousal and valence levels are discriminated simultaneously using a parallel structure, as shown in Fig. 6(b).

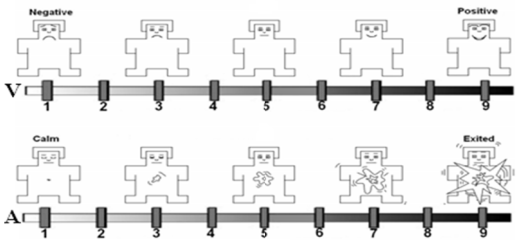

Fig. 7. 2-D SAM questionnaire [57].

III. Experimental Design

The performance of the proposed neural network is investigated using the EEG data collected from healthy subjects. The experimental design in the collection of EEG data is described in this section.

A. Emotion Elicitation

Studies have shown that elicitor (subject elicited versus event elicited), setting (controlled condition in the lab versus real world), focus (expression versus perception), and subject awareness (open recording versus hidden recording) are the factors that can influence the emotion elicitation results [17]. Subject elicited category refers to the instruction given to the subject for expressing a specific emotion (e.g., to mimic the facial expression of happiness), or recalling the past emotional episodes. Event elicited category refers to the use of some images, sounds, video clips, or any emotionally evocative stimuli. The International Affective Picture System (IAPS) [33], International Affective Digitized Sound (IADS) system [58], Bernard Bouchard's synthesized musical clips [59], and Gross and Levenson's movie clips [60] are used to elicit emotional response. Although touch, smell, and taste are also known to influence human emotion, these are less studied in [61] and thus are not used in this paper.

In this study, a combination of arousing pictures from IAPS (1022, 1026, 1052, 1110, 1200, 1220, 1920, 1932, 2030, 2040, 2071, 2141, 2165, 2205, 2276, 2312, 2340, 2345, 2530, 2700, 2900, 3530, 5711, 5720, 5779, 5780, 5800, 5811, 5814, 5836, 6010, 6821, 6834, 6836, 6838, 6840, 6940, 8120, 8350, 8461, 8497, 9220, 9530) and synthesized musical excerpts belonging to Bernard Bouchard are used to elicit emotional responses from the subjects. These data are generally accompanied by affective evaluations from the experts or average judgments of several people. The emotional feeling or perception from a stimulus, however, differs from subject to subject based on the subject's experience.

Therefore, even though predefined evaluation labels are available, the SAM questionnaire is used in this paper to rate the subjects' emotions. An example of the SAM questionnaire is shown in Fig. 7.

B. Experimental Protocol

The duration of emotion elicited can be categorized into three categories: full blown emotions that last from seconds to minutes, moods that last from minutes to hours, and emotional disorders that last for years or an entire lifetime [14]. Ideally, an emotion recognition system should be able to discriminate the emotional states from the EEG as fast as possible [62]. Hence, this paper focuses on full blown emotions whereby the emotional stimuli are presented for 1 min in a counterbalanced and random order. The protocol of the experiment is shown in Fig. 8.

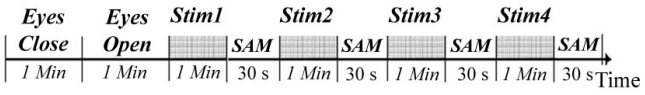

Fig. 8. Paradigm for intersubjects experiment.

The data are collected with subjects seated in a comfortable chair in a registration room whereby the experimental procedure is explained to them. The subjects are then asked to fill in a handedness questionnaire [63]. The EEG is recorded using the BIMEC from Brainmarker BV. The BIMEC has one reference channel plus eight EEG channels with a sampling rate of 250 Hz. The impedance of the Ag/AgCl electrodes is kept <10 kΩ. Considering the cerebral lateralization during emotional perception [64], the eight Ag/AgCl electrodes are attached bilaterally on the subjects' scalps using the 10/20 system of electrode placement, as shown in Fig. 6(a), where the Cz is the reference channel [65]. EEG data are collected for a 6-min period that comprised of 1-min eyes closed, 1-min eyes open, and 1 min for four emotional stimuli. The eyes-closed and eyes-open resting states are applied to bring all the subjects back to a similar mental state. The subjects are exposed to four emotional stimuli in different arousal and valence levels. The visual stimuli are displayed on a 19-inch monitor positioned 1 m far from the participant's eyes and the audio stimuli are played by the speakers with a constant output power. The categories of emotional stimuli are presented randomly such that each stimulus category is observed one time for every subject.

C. Subjects

EEG data were collected from 57 healthy subjects (age: 17–33, nine women and 48 men).

The valence and arousal levels measured from SAM questionnaire are used for labeling the EEG data. The valence and arousal levels provide a dynamic representation of the emotional states. The valence–arousal plane provides a dynamic representation of the emotional states. The valence and arousal levels are evaluated separately. The boundaries between different classes are determined from the subjects' answers to the SAM questionnaire. Negative emotions are labeled when Valence ≤ 3 and positive emotions are labeled when Valence ≥ 7. Calm emotions are labeled when Arousal ≤ 3 and excited emotions are labeled when Arousal ≥ 7. For example, the subjects with SAM responses if Valence ≤ 3 are labeled as negative whereas subjects with Valence ≥ 7 are labeled as positive.

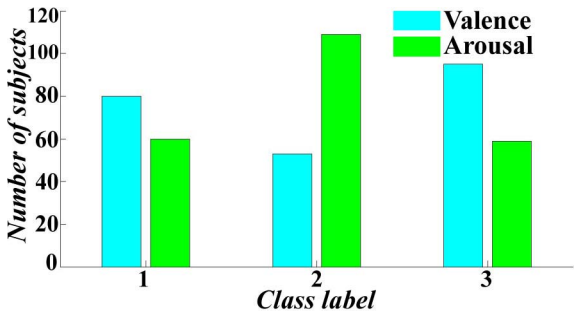

Fig. 9. Population of classes in each group.

IV. Experimental Results and Discussion

It was explained in previous sections that the emotional states are recognized based on the valence and arousal levels in this paper. The negative and positive states from valence dimension and calm and highly exited states from arousal dimension are investigated in classes 1 and 3. The EEG signals are acquired during watching audio–visual stimuli through an explained paradigm. The subjects' emotional states are scored using SAM questionnaire. The collected EEG signals are then labeled with SAM responses. Subsequently, accuracy of the proposed biological inspired network is checked using this data. A single-trial EEG data of 1 s is used to test the proposed neural network and classification accuracy of the network for valence/arousal level identification is computed. A 5-fold cross-validation method is then applied to validate the results. Nevertheless, performance of the proposed network is evaluated using other trials with size of 1 s as well. Average and standard deviation of classification accuracies calculated for all trials using the proposed network is shown in Table II.

The cross-validation method assesses how the results generated by the methods will generalize to an independent dataset. In 5-fold cross-validation method, 1/5 of the observation from the original sample set is used as the testing data, and the remaining observations are used as the training data. The partitions are generated using the cvpartition function in the MATLAB Bioinformatics toolbox. The population size of arousal and valence categories are shown in Fig. 9 where the classes' populations are $n_v = 175(c_{1v} = 80, c_{3v} = 95)$ and $n_a = 119(c_{1a} = 60, c_{3a} = 59)$.

The input of neural network is the normalized EEG data in range 0–1. The normalization is done to remove the dc component of EEG signal and it is done for each subject separately. Every individual element of each subject (EEG sample points of each channel) is divided by square root of summation of square of all its elements (EEG sample points of all channels acquired at the same time) as given in

$$x_i(n) = \frac{x_i^{'}(n)}{\sqrt{\sum_{i=1}^{n_c} x_i^{'2}(n)}}, x_i(n) \in [0, 1]. \tag{23}$$

The proposed neural network has four variable parameters including N, n_{out}, n_{h}, and σ. The maximum number of hidden neurons is set to $n_{\text{h}} = 2n_{\text{a}}$ for arousal level recognition and $2n_{\text{v}}$ for valence level recognition. Because the network with optimum parameters is appreciated and considering the fixed topology of the network, a straightforward approach is to apply a GA as an optimization tool to compute the optimum n_{out}, σ, and N.

The GA is an optimization algorithm, which is invented based on genetics and evolution. Usually, the initial population of individuals is generated randomly. After, the fitness function, which is a measure of improvement of approximation, is calculated for each individual. Then, crossover and mutation are performed on the selected individuals to create a new individual that replaces the worst members of the population offspring. These procedures are continued until the end condition is satisfied [68].

In this paper, the classification accuracy of network is considered as a fitness function with population initial range of [250 1000], [1 100], and [0.01 10] for N, n_{out}, and σ, respectively. The fraction rate for crossover is 0.8 in a scattered format with applying an adaptive feasible method as the mutation function. Population size is 20 and maximum generation is 100. The programming is done using global optimization toolbox in MATLAB. According to GA results, the N, n_{out}, and σ are set to 256, 12, and 3.28, respectively. The classification accuracies shown in Table II are computed using the optimum parameters.

In addition, for comparison reasons, different feature extraction techniques from EEG data for emotion recognition are implemented. The extracted features are then classified using different feedforward methods including NB, KNN, and ELM with a sigmoid output function. The results are shown in Table II, where the FBM denotes fractional brownian motion [69]–[72], Hjorth [66] explains the Hjorth parameters including activity, mobility, and complexity. Furthermore, two recently applied feature extraction techniques including the wavelet transform and zero-order crossing are also implemented. The HOC presents the higher order zero crossing method that has been used in [50] and the W_C denotes the wavelet-based features that has been applied in [51] for EEG-based emotion recognition. Murugappan *et al.* [51] have employed the discrete wavelet transform for five scales using the daubechies fourth-order orthonormal bases and the extracted wavelet coefficients at the [1, 2, 3, 4, 5]th scales that correspond to the alpha, beta, and gamma bands to estimate the wavelet energy-based features called recoursing energy efficiency, its modified form namely logarithmic REE and absolute logarithmic REE. To have a fair comparison, both methods are, however, tested either in the frequency ranges that have been selected in their papers (8–30 Hz) and (4–68 Hz) or in our selected frequency range (4–40 Hz).

On the other hand, the ERNN computes the MSCE features between different brain regions at different frequencies ranged in 4 and 40 Hz. Subsequently, it is very important to know what are the most effective EEG channels and the most effective frequencies for valence/arousal level recognition from EEG data. This task is performed automatically by doing the feature ranking. Nevertheless, to bright up the most effective features, the first 1000 ranked features are selected.

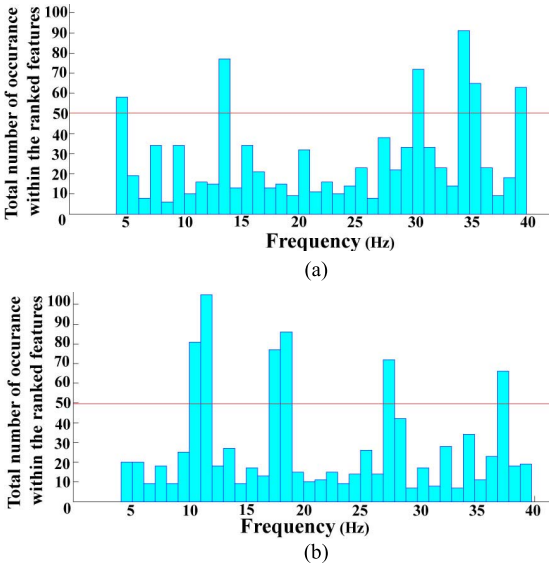

Fig. 10. Distribution of effective frequencies for (a) valence level recognition and (b) arousal level recognition.

TABLE III
EFFECTIVE EEG CHANNELS FOR VALENCE LEVEL RECOGNITION

Effective frequency (Hz)	Effective Channel	
	Channel i	*Channel j*
4-5	F_3	$C3$, C_4 (1/3 C3)
13-14	$C3$, C_4 (1/5 C3)	F_3
30-31	P_4	T_7
34-46	T_7	P_4,T_8
39-40	T_8	T_7

TABLE IV
EFFECTIVE EEG CHANNELS FOR AROUSAL LEVEL RECOGNITION

Effective frequency (Hz)	Effective Channel	
	Channel i	*Channel j*
10-12	C_4	F_4, P_4
17-18	F_3	T_8
27-28	P_4	C_4
37-38	T_8	F_3

Fig. 10(a) and Fig. 10(b) shows the frequency distribution of the most effective features for valence and arousal recognition, respectively.

The results shown in Fig. 10(a) and (b) suggest that the 4–5 Hz of theta band, the 13–14 Hz of alpha band, the 30–31 Hz of upper beta band and 34–36 Hz, and 39–40 Hz in lower gamma band are more effective for recognition of negative versus positive emotions from EEG signal using the MSCE features. Furthermore, the MSCE features at 10–12 Hz upper alpha band and 17–18 Hz, and 27–28 Hz of beta band 37–38 Hz of gamma band are more useful for recognition of arousal level using MSCE features. Since the population of all features is 1000, the red line in Fig. 10 shows the P_value $\geq$ 0.05. In addition, a better conclusion can be made when the effective channels at these frequencies are provided, as shown in Tables III and IV.

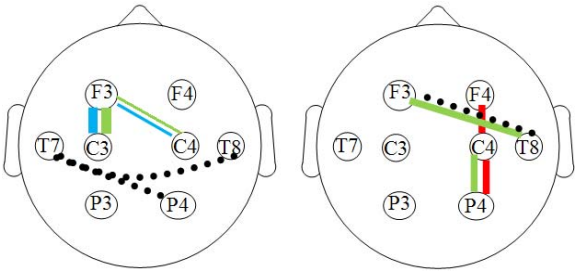

Fig. 11. Most effective connectivity features for (left) valence and (right) arousal level discrimination.

The results presented in Table III show that the perception of valence level of emotional stimuli are more detectable based on functional connectivity between left frontal region (F_3) and central regions (C3, C_4) of the brain at lower EEG frequencies (theta and alpha bands) or based on functional connectivity between parietal (P_4) and temporal regions (T_7, T_8) at upper EEG frequencies (beta and gamma bands).

The results in Table IV also show that during perception of arousal level of emotional stimuli, more amount of changes will happen at functional connectivity between right central region (C_4) and right frontal (F_4) and parietal regions (P_4) at lower EEG frequencies (alpha band). Furthermore, changes in arousal level of stimuli causes more changes in functional connectivity between right parietal (P_4) and right central regions (C_4), and right temporal (T_8) and left frontal (F_3) regions at upper EEG frequencies (beta and gamma bands).

The demonstrated results in Tables III and IV are graphically shown in Fig. 11. The connectivity in different frequencies has been highlighted in different colors. The blue line shows the theta band, the red line shows the alpha band, the green line shows the beta band, and black dashed line shows to the lower gamma band.

It can be concluded from the results that brain has different policies (functional connectivity patterns) for the recognition of valence and arousal level of the emotion. This phenomenon would be very useful in applications such as the improvement of the brain plasticity [73], [74] or the investigation of brain aging using various types of stimuli. There are evidences for a global posterior–anterior shift in aging [75]. It should be noted that these results are, however, based on eight EEG channels and using audio–visual stimulus.

Furthermore, obtaining the network parameters using other adaptive methods such as [76]–[78] should be considered instead of using GA algorithm for optimizing them. However, as is shown in Table II, the mutual information does not lead to a good network performance, therefore, looking for a better adaptive method is suggested in the future works.

V. CONCLUSION

This paper presents a biological inspired feedforward neural network discriminating emotion from EEG based on valence and arousal levels. The EEG data from the perception of emotional stimuli in healthy participants are collected. The top-down approach is formulated and bottom-up approach is bypassed using SAM answers. Subsequently, the performance

of the proposed neural network for discriminating emotions is evaluated using the EEG data and SAM responses. The results show that there are patterns of brain regions connectivity in the perception of individual emotional stimuli. These patterns are detectable by estimating the connectivity between different brain regions from the EEG data. However, these patterns vary in different subjects but common patterns can be selected at specific frequencies. Nevertheless, the feedforward architecture is presented by considering a constant level of attention, mood, and mental health for all the subjects. Therefore, further assessment for understanding the impact of attention level, moods, and mental disorders on the perception of emotional stimuli should be done. In addition, improvement of the network for a multiclass valence/arousal problem is proposed for future works.

ACKNOWLEDGMENT

The authors would like to thank M. Heijnen and S. W. Tan for their support in the data collection of the experiment and B. Crüts for his valuable advice on designing the experiment.

REFERENCES

[1] R. W. Picard, *Affective Computing*. Cambridge, MA, USA: MIT Press, 2000.

[2] P. Ekman, "Facial expression and emotion," *Amer. Psychol.*, vol. 48, no. 4, pp. 384–392, 1993.

[3] T. Baumgartner, M. Esslen, and L. Jäncke, "From emotion perception to emotion experience: Emotions evoked by pictures and classical music," *Int. J. Psychophysiol.*, vol. 60, no. 1, pp. 34–43, 2006.

[4] M. L. Phillips, "Understanding the neurobiology of emotion perception: Implications for psychiatry," *Brit. J. Psychiatry*, vol. 182, no. 3, pp. 190–192, 2003.

[5] R. Adolphs, H. Damasio, D. Tranel, and A. R. Damasio, "Cortical systems for the recognition of emotion in facial expressions," *J. Neurosci.*, vol. 16, pp. 7678–7687, Dec. 1996.

[6] J. G. Taylor, K. Scherer, and R. Cowie, "Emotion and brain: Understanding emotions and modelling their recognition," *Neural Netw.*, vol. 18, no. 4, pp. 313–316, 2005.

[7] K. Oatley and P. N. Johnson-Laird, "Towards a cognitive theory of emotions," *Cognit. Emot.*, vol. 1, no. 1, pp. 29–50, 1987.

[8] R. Khosrowabadi, Q. Hiok Chai, A. Wahab, and A. Kai Keng, "EEG-based emotion recognition using self-organizing map for boundary detection," in *Proc. 20th ICPR*, Istanbul, Turkey, Aug. 2010, pp. 4242–4245.

[9] J. Lin, M. Spraragen, J. Blythe, and M. Zyda, "EmoCog: Computational integration of emotion and cognitive architecture," presented at the 24th Int. Florida Artificial Intelligence Research Society Conf., Palm Beach, FL, USA, 2011.

[10] R. Khosrowabadi, M. Heijnen, A. Wahab, and Q. H. Chai, "The dynamic emotion recognition system based on functional connectivity of brain regions," in *Proc. IEEE Intell. Veh. Symp.*, Jun. 2010, pp. 377–381.

[11] R. Khosrowabadi and A. Wahab bin Abdul Rahman, "Classification of EEG correlates on emotion using features from Gaussian mixtures of EEG spectrogram," in *Proc. Int. Conf. Inf. Commun. Technol. Muslim World*, Dec. 2010, pp. E102–E107.

[12] A. Wahab, N. Kamaruddin, L. K. Palaniappan, M. Li, and R. Khosrowabadi, "EEG signals for emotion recognition," *J. Comput. Methods Sci. Eng.*, vol. 10, pp. 1–11, Sep. 2010.

[13] R. Khosrowabadi, "Modelling of emotions based on EEG signal," Ph.D. dissertation, School Comput. Eng., Nanyang Technol. Univ., Singapore, 2012.

[14] R. Cowie and R. R. Cornelius, "Describing the emotional states that are expressed in speech," *Speech Commun.*, vol. 40, nos. 1–2, pp. 5–32, 2003.

[15] R. Khosrowabadi, A. Wahab, K. K. Ang, and M. H. Baniasad, "Affective computation on EEG correlates of emotion from musical and vocal stimuli," in *Proc. IJCNN*, Atlanta, GA, USA, Jun. 2009, pp. 1168–1172.

[16] J. Kim and E. Andre, "Emotion recognition based on physiological changes in music listening," *IEEE Trans. Pattern Anal. Mach. Intell.*, vol. 30, no. 12, pp. 2067–2083, Dec. 2008.

[17] R. W. Picard, E. Vyzas, and J. Healey, "Toward machine emotional intelligence: Analysis of affective physiological state," *IEEE Trans. Pattern Anal. Mach. Intell.*, vol. 23, no. 10, pp. 1175–1191, Oct. 2001.

[18] M. Pantic and L. J. M. Rothkrantz, "Automatic analysis of facial expressions: The state of the art," *IEEE Trans. Pattern Anal. Mach. Intell.*, vol. 22, no. 12, pp. 1424–1445, Dec. 2000.

[19] J. C. Borod and N. K. Madigan, "Neuropsychology of emotion and emotional disorders: An overview and research directions," in *Neuropsychology of Emotion*, J. C. Borod, Ed. New York, NY, USA: Oxford Univ. Press, 2000, pp. 3–28.

[20] S. G. Costafreda, M. J. Brammer, A. S. David, and C. H. Y. Fu, "Predictors of amygdala activation during the processing of emotional stimuli: A meta-analysis of 385 PET and fMRI studies," *Brain Res. Rev.*, vol. 58, no. 1, pp. 57–70, 2008.

[21] T. Canli, Z. Zhao, J. E. Desmond, E. Kang, J. Gross, and J. D. E. Gabrieli, "An fMRI study of personality influences on brain reactivity to emotional stimuli," *Behavioral Neurosci.*, vol. 115, no. 1, pp. 33–42, 2001.

[22] R. Adolphs, "Neural systems for recognizing emotion," *Current Opinion Neurobiol.*, vol. 12, no. 2, pp. 169–177, 2002.

[23] R. H. Hall. (1998). *Explicit and Implicit Memory* [Online]. Available: http://web.mst.edu/~rhall/neuroscience/

[24] H. Kober, L. F. Barrett, J. Joseph, E. Bliss-Moreau, K. Lindquist, and T. D. Wager, "Functional grouping and cortical–subcortical interactions in emotion: A meta-analysis of neuroimaging studies," *NeuroImage*, vol. 42, no. 2, pp. 998–1031, 2008.

[25] M. D. Lewis and R. M. Todd, "The self-regulating brain: Cortical-subcortical feedback and the development of intelligent action," *Cognit. Develop.*, vol. 22, no. 4, pp. 406–430, 2007.

[26] G. C. De Angelis, I. Ohzawa, and R. D. Freeman, "Receptive-field dynamics in the central visual pathways," *Trends Neurosci.*, vol. 18, no. 10, pp. 451–458, 1995.

[27] E. D. Jarvis, O. Gunturkun, L. Bruce, A. Csillag, H. Karten, W. Kuenzel, L. Medina, G. Paxinos, D. J. Perkel, T. Shimizu, G. Striedter, J. M. Wild, G. F. Ball, J. Dugas-Ford, S. E. Durand, G. E. Hough, S. Husband, L. Kubikova, D. W. Lee, C. V. Mello, A. Powers, C. Siang, T. V. Smulders, K. Wada, S. A. White, K. Yamamoto, J. Yu, A. Reiner, and A. B. Butler, "Avian brains and a new understanding of vertebrate brain evolution," *Nature Rev. Neurosci.*, vol. 6, pp. 151–159, Feb. 2005.

[28] E. R. Kandel, *In Search of Memory: The Emergence of a New Science of Mind*. New York, NY, USA: Norton, 2007.

[29] K. N. Ochsner and J. J. Gross, "The neural architecture of emotion regulation," in *Handbook of Emotion Regulation*, J. J. Gross, Ed. New York, NY, USA: Guilford Press, 2009, pp. 87–109.

[30] T. Brosch, G. Pourtois, and D. Sander, "The perception and categorisation of emotional stimuli: A review," *Cognit. Emot.*, vol. 24, no. 3, pp. 377–400, 2010.

[31] K. R. Scherer, A. Schorr, and T. Johnstone, *Appraisal Processes in Emotion*. New York, NY, USA: Oxford Univ. Press, 2001.

[32] E. T. Rolls, *The Brain and Emotion*. New York, NY, USA: Oxford Univ. Press, 1999.

[33] P. J. Lang, M. M. Bradley, and B. N. Cuthbert, "International affective picture system (IAPS): Affective ratings of pictures and instruction manual," Dept. Nat. Inst. Mental Health Center Emotion Attention, Univ. Florida, Gainesville, FL, USA, Tech. Rep. A-6, 2005.

[34] M. Esslen, R. D. Pascual-Marqui, D. Hell, K. Kochi, and D. Lehmann, "Brain areas and time course of emotional processing," *NeuroImage*, vol. 21, no. 4, pp. 1189–1203, 2004.

[35] J. Kim, *Philosophy of Mind*, 3rd ed. Boulder, CO, USA: Westview, 2010.

[36] J. Musch and K. C. Klauer, *The Psychology of Evaluation: Affective Processes in Cognition and Emotion*. New York, NY, USA: Taylor & Francis, 2003.

[37] O. Sporns, "Brain connectivity," *Scholarpedia*, vol. 2, no. 10, p. 4695, 2007.

[38] S. M. Kay, *Modern Spectral Estimation: Theory and Application*. Englewood Cliffs, NJ, USA: Prentice-Hall, 1988.

[39] G. Carter, C. Knapp, and A. Nuttall, "Estimation of the magnitude-squared coherence function via overlapped fast Fourier transform processing," *IEEE Trans. Audio Electroacoust.*, vol. 21, no. 4, pp. 337–344, Aug. 1973.

[40] R. Zass and A. Shashua, "Nonnegative sparse PCA," in *Advances in Neural Information Processing Systems*, vol. 19, B. Schölkopf, J. Platt, and T. Hoffman, Eds. Cambridge, MA, USA: MIT Press, 2007.

[41] A. J. Flugge, S. Olhede, and M. Fitzgerald, "Non-negative PCA for EEG-data analysis," *Interpreting*, vol. 101, pp. 776–780, Apr. 2009.
[42] S. Chen, C. F. N. Cowan, and P. M. Grant, "Orthogonal least squares learning algorithm for radial basis function networks," *IEEE Trans. Neural Netw.*, vol. 2, no. 2, pp. 302–309, Mar. 1991.
[43] H. Demuth and M. Beale, *Neural Network Toolbox for use with Matlab*. Natick, MA, USA: MathWorks, 1998.
[44] J. Park and I. W. Sandberg, "Universal approximation using radial-basis-function networks," *Neural Comput.*, vol. 3, no. 2, pp. 246–257, 1991.
[45] G.-B. Huang, Q.-Y. Zhu, and C.-K. Siew, "Extreme learning machine: Theory and applications," *Neurocomputing*, vol. 70, nos. 1–3, pp. 489–501, 2006.
[46] P. D. Wasserman, *Advanced Methods in Neural Computing*. New York, NY, USA: Wiley, 1993.
[47] T. Cover and P. Hart, "Nearest neighbor pattern classification," *IEEE Trans. Inf. Theory*, vol. 13, no. 1, pp. 21–27, Jan. 1967.
[48] W. J. Krzanowski, *Principles of Multivariate Analysis: A User's Perspective*. New York, NY, USA: Oxford Univ. Press, 2000.
[49] N. Cristianini and J. Shawe-Taylor, *An Introduction to Support Vector Machines and Other Kernel-Based Learning Methods*. Cambridge, U.K.: Cambridge Univ. Press, 2000.
[50] P. C. Petrantonakis and L. J. Hadjileontiadis, "Emotion recognition from EEG using higher order crossings," *IEEE Trans. Inf. Technol. Biomed.*, vol. 14, no. 2, pp. 186–197, Mar. 2010.
[51] M. Murugappan, N. Ramachandran, and Y. Sazali, "Classification of human emotion from EEG using discrete wavelet transform," *J. Biomed. Sci. Eng.*, vol. 3, pp. 390–396, Apr. 2010.
[52] A. Ortony and T. J. Turner, "What's basic about basic emotions?" *Psychol. Rev.*, vol. 97, no. 3, pp. 315–331, 1990.
[53] P. Ekman, "Basic emotions," in *Handbook of Cognition and Emotion*, T. Dagleish and M. Power Eds. New York, NY, USA: Wiley, 1999, pp. 45–60.
[54] C. E. Izard, *Human Emotions*. New York, NY, USA: Plenum, 1977.
[55] R. Plutchik, "A general psychoevolutionary theory of emotion," in *Emotion: Theory, Research, and Experience*. vol. 1, R. Plutchik and H. Kellerman, Eds. New York, NY, USA: Academic, 1980, pp. 3–33.
[56] J. A. Russell, "A circumplex model of affect," *J. Personality Soc. Psychol.*, vol. 39, no. 6, pp. 1161–1178, 1980.
[57] P. J. Lang, "Behavioral treatment and bio-behavioral assessment: Computer applications," in *Technology in Mental Health Care Delivery Systems*, J. Sidowski, J. Johnson, and T. Williams, Eds. Norwood, NJ, USA: Ablex, 1980, pp. 119–137.
[58] M. M. Bradley and P. J. Lang, "The international affective digitized sounds (2nd edition; IADS-2): Affective ratings of sounds and instruction manual," Dept. Nat. Inst. Mental Health Center Emotion Attention, Univ. Florida, Gainesville, FL, USA, Tech. Rep. B-3, 2007.
[59] S. Vieillard, I. Peretz, N. Gosselin, S. P. Khalfa, L. Gagnon, and B. Bouchard, "Happy, sad, scary and peaceful musical excerpts for research on emotions," *Cognit. Emot.*, vol. 22, no. 4, pp. 720–752, 2008.
[60] J. J. Gross and R. W. Levenson, "Emotion elicitation using films," *Cognit. Emot.*, vol. 9, no. 1, pp. 87–108, 1995.
[61] V. V. Kulish, A. I. Sourin, and O. Sourina, "Fractal spectra and visualization of the brain activity evoked by olfactory stimuli," presented at the the 9th Asian Symp. on Visualization, Hong Kong, 2007.
[62] G. Chanel, J. J. M. Kierkels, M. Soleymani, and T. Pun, "Short-term emotion assessment in a recall paradigm," *Int. J. Human-Comput. Stud.*, vol. 67, no. 8, pp. 607–627, 2009.
[63] R. C. Oldfield, "The assessment and analysis of handedness: The Edinburgh inventory," *Neuropsychologia*, vol. 9, no. 1, pp. 97–113, 1971.
[64] P. Fusar-Poli, A. Placentino, F. Carletti, P. Allen, P. Landi, M. Abbamonte, F. Barale, J. Perez, P. McGuire, and P. L. Politi, "Laterality effect on emotional faces processing: ALE meta-analysis of evidence," *Neurosci. Lett.*, vol. 452, no. 3, pp. 262–267, 2009.
[65] R. W. Thatcher, C. J. Biver, and D. North, "EEG coherence and phase delays: Comparisons between single reference, average reference and current source density," Univ. South Florida College of Medicine, Tampa, FL, USA, Tech. Rep. A-1, Jun. 2004.
[66] B. Hjorth, "EEG analysis based on time domain properties," *Electroencephalogr. Clin. Neurophysiol.*, vol. 29, no. 3, pp. 306–310, 1970.
[67] R. Khosrowabadi, C. Quek, K. K. Ang, S. W. Tung, and M. Heijnen, "A brain-computer interface for classifying EEG correlates of chronic mental stress," presented at the IEEE Int. Joint Conf. on Neural Networks, San Jose, CA, USA, 2011.
[68] D. Whitley, "Genetic algorithms and neural networks," in *Genetic Algorithms in Engineering and Computer Science*, vol. 3, J. Periaux and G. Winter, Eds. New York, NY, USA: Wiley, 1995, pp. 203–216.
[69] J. Beran, *Statistics for Long-Memory Processes*, vol. 61. Gainesville, FL, USA: Chapman & Hall, 1994.
[70] P. Flandrin, "Wavelet analysis and synthesis of fractional Brownian motion," *IEEE Trans. Inf. Theory*, vol. 38, no. 2, pp. 910–917, Mar. 1992.
[71] J. Istas and G. Lang, "Quadratic variations and estimation of the local Hölder index of a Gaussian process," *Ann. l'Institut Henri Poincare B, Probab. Stat.*, vol. 33, pp. 407–436, 1997.
[72] P. Abry, P. Flandrin, M. S. Taqqu, and D. Veitch, "Self-similarity and long-range dependence through the wavelet lens," in *Theory and Applications of Long-Range Dependence*, P. Doukhan, G. Oppenheim, and M. S. Taqqu, Eds. Boston, MA, USA: Birkhauser, 2000, pp. 527–556.
[73] J. Doyon and H. Benali, "Reorganization and plasticity in the adult brain during learning of motor skills," *Current Opin. Neurobiol.*, vol. 15, no. 2, pp. 161–167, 2005.
[74] H. W. Mahncke, A. Bronstone, and M. M. Merzenich, "Brain plasticity and functional losses in the aged: Scientific bases for a novel intervention," in *Progress in Brain Research*. vol. 157, R. M. Aage, Ed. New York, NY, USA: Elsevier, 2006, pp. 81–109.
[75] S. W. Davis, N. A. Dennis, S. M. Daselaar, M. S. Fleck, and R. Cabeza, "Qué PASA? The posterior–anterior shift in aging," *Cerebral Cortex*, vol. 18, no. 5, pp. 1201–1209, May 2008.
[76] P. C. Petrantonakis and L. J. Hadjileontiadis, "Adaptive extraction of emotion-related EEG segments using multidimensional directed information in time-frequency domain," in *Proc. Annu. Int. Conf. IEEE EMBC*, Aug./Sep. 2010, pp. 1–4.
[77] M. Arvaneh, G. Cuntai, K. K. Ang, and C. Quek, "Optimizing spatial filters by minimizing within-class dissimilarities in electroencephalogram-based brain–computer interface," *IEEE Trans. Neural Netw. Learn. Syst.*, vol. 24, no. 4, pp. 610–619, Apr. 2013.
[78] R. Zhang, Y. Lan, G.-B. Huang, and Z.-B. Xu, "Universal approximation of extreme learning machine with adaptive growth of hidden nodes," *IEEE Trans. Neural Netw. Learn. Syst.*, vol. 23, no. 2, pp. 365–371, Feb. 2012.

Reza Khosrowabadi (S'09) received the B.Sc. degree in biomedical engineering from the Sahand University of Technology, Sahand, Iran, and the Ph.D. degree in computer science from Nanyang Technological University, Singapore.

He is currently a Post-Doctoral Research Fellow with Duke-NUS Graduate Medical School, Singapore. He was a Student Member of the Brain-Computer Interface Laboratory, Institute for Infocomm Research, Agency for Science, Technology and Research, Singapore, from 2008 to 2010. He was an Application Engineer with Akbarieh Co. (Roche Agency, Diagnostics Department), Tehran, Iran, from 2004 to 2007. His current research interests include multimodal neuroimaging, signal processing, machine learning, pattern recognition, and cognitive science.

Chai Quek (M'96–SM'10) received the B.Sc. degree in electrical and electronics engineering and the Ph.D. degree in intelligent control from Heriot-Watt University, Edinburgh, U.K.

He is currently an Associate Professor, a member of the Center for Computational Intelligence (formerly the Intelligent Systems Laboratory), and the Assistant Chair with the School of Computer Engineering, Nanyang Technological University, Singapore. His current research interests include intelligent control, intelligent architectures, artificial intelligence in education, neural networks, fuzzy neural systems, neurocognitive informatics, and genetic algorithms.

Dr. Quek is a member of the IEEE Technical Committee on Computational Finance and Economics.

Kai Keng Ang (S'05–M'07) received the B.A.Sc. (Hons.) and Ph.D. degrees in computer engineering from Nanyang Technological University, Singapore.

He is currently the Brain-Computer Interface Laboratory Head and a Scientist with the Institute for Infocomm Research, Agency for Science, Technology and Research, Singapore. He was a Senior Software Engineer with Delphi Automotive Systems Singapore Pte. Ltd., Singapore, from 1999 to 2003, where he was involved in research on embedded software for automotive engine controllers. He has authored or co-authored several papers. His current research interests include brain–computer interfaces, computational intelligence, machine learning, pattern recognition, and signal processing.

Abdul Wahab (M'89) received the Degree from the University of Essex, Essex, U.K., in 1979, the M.Sc. degree from the National University of Singapore, Singapore, in 1987, and the Ph.D. degree from Nanyang Technological University, Singapore.

His research has been in the areas of telecommunication, signal processing, and artificial intelligence. He was with Hewlett Packard Singapore, Singapore, as a Research and Development Project Manager both in CO, USA. He joined Nanyang Technological University in 1990, where he was an Associate Professor, before joining the International Islamic University of Malaysia, Malaysia, as a Professor, in 2009. He has authored over 100 conference papers, journal papers, patents, and book chapters in the areas of digital and optical computing, signal processing, and artificial intelligence.